Real-time Hyperspectral Imaging for Non-invasive Monitoring of Tissue Ischemia

Anoek Strumane[1,*], Jens D. Winne[1], Danilo Babin[1], Jan Aelterman[1,2], Hiep Luong[1] and Wilfried Philips[1]

[1]Department of Telecommunications and Information Processing (TELIN) - IPI Research Group, Ghent University-imec, 9000 Ghent, Belgium
[2]Department of Physics and Astronomy, Ghent University, 9000 Ghent, Belgium
*anoek.strumane@ugent.be

***Abstract*—This paper presents a study on the use of hyperspectral imaging (HSI) for non-invasive, real-time monitoring of skin ischemia. We propose a novel ischemia index based on reflectance in a limited number of wavelengths, which can be calculated and visualized in real-time with low memory requirements. The index is tested on hyperspectral images of healthy and ischemic forearms, obtained by performing lower arm occlusion, and is compared to five other state-of-the-art indices from literature using binary support vector machines (SVMs). The results show that the proposed index is able to robustly distinguish between healthy and ischemic tissue in real-time, thus highlighting their potential to be used in a clinical setting.**

***Keywords*—Ischemia, Hyperspectral imaging, Snapshot camera, Real-time**

I. INTRODUCTION

Adequate blood supply is essential for cell homeostasis and metabolism. Skin ischemia, in which blood supply to part of skin tissue is restricted, leads to tissue hypoxia limiting these essential mechanisms. Monitoring of ischemic conditions provides information of, for example, tissue states during surgery [1], monitoring of wound healing [2] and assessment of peripheral arterial disease [3]. Classical methods such as oximeters [4], blood gas analysis, diffuse reflectance spectroscopy [5], and angiography [6] are often invasive, require skin contact or contrast agents, and often only provide local measurements.

HSI has proven capable of detecting tissue ischemia without the need for invasive procedures [7]. However, current HSI methods have poor temporal resolution, limiting real-time feedback. Recent advances in snapshot cameras have made it possible to acquire the complete spectrum in one instance, enabling real-time monitoring. While HSI shows potential, current methods are often complex and computationally expensive, requiring a large amount of training data. Hence, they are often built on simulated data using (multi-layered) Monte Carlo simulations on a skin model [8], [9].

We hypothesize that a limited number of wavebands can detect skin tissue ischemia, reducing the computational demand and possibly increasing the diagnostic accuracy. A novel ischemia index based on light reflectance in a small number of wavebands is proposed, and real-time ischemia maps are calculated with low memory requirement. We use a dual snapshot system to optimize the spectral domain and highlight the real-time capabilities. The index is tested on hyperspectral images of the upper arm and compared two five other state of the art ischemia indices.

II. METHODOLOGY

A. Camera Setup

IMEC's snapshot UAV VIS+NIR camera (Imec, Belgium) was used in this study, consisting of two separate snapshot mosaic cameras with Fabry-Pérot interference filter arrays in the same housing. The first camera will be referred to as the VIS camera and the second as the NIR camera. The cameras have a spectral range of 459-590 nm and 605-841 nm respectively. Both cameras have a resolution of 272x512 pixels and a full width at half maximum of about 10 nm. Together they record 31 spectral bands. The camera was mounted at a height of 50 cm, and both a halogen desk lamp and LED bars (Effilux, France) were used as the light sources in the camera's spectral range.

B. Measurement Protocol

To obtain hyperspectral images of ischemic skin tissue, 14 human test subjects had their upper arm occluded for five minutes using a pressure cuff, ensuring arterial and venous occlusion [8]. The skin colour of the test subjects ranged from I to IV on the Fitzpatrick scale. The first experiment used the desk lamp and included 12 test subjects of whom four images were taken, two (palmar and dorsal side of the upper arm) before cuffing and two during cuffing (after 5 minutes of cuffing), resulting in one VIS and one NIR hypercube per image. Using the LED bars, a second experiment included two test subjects of which one image was taken of the dorsal side before cuffing and one during cuffing.

C. Preprocessing

Figure 1 shows the complete processing pipeline. To correct for non-uniformity, dark-corrected images were normalized using a white reference measurement (Spectralon, SphereOptics GmbH). The normalized hypercubes were then segmented by applying Canny edge detection followed by a flood fill to exclude background pixels. The VIS and NIR hypercubes were then registered using the SimpleITK rigid registration method. The hypercubes were divided into 250 superpixels using SLIC algorithm [10], using the various wavebands as the color space of the images. Each slice of the resulting hypercube corresponds to a map of superpixels, where each superpixel is the mean reflectance value of all pixels within it.

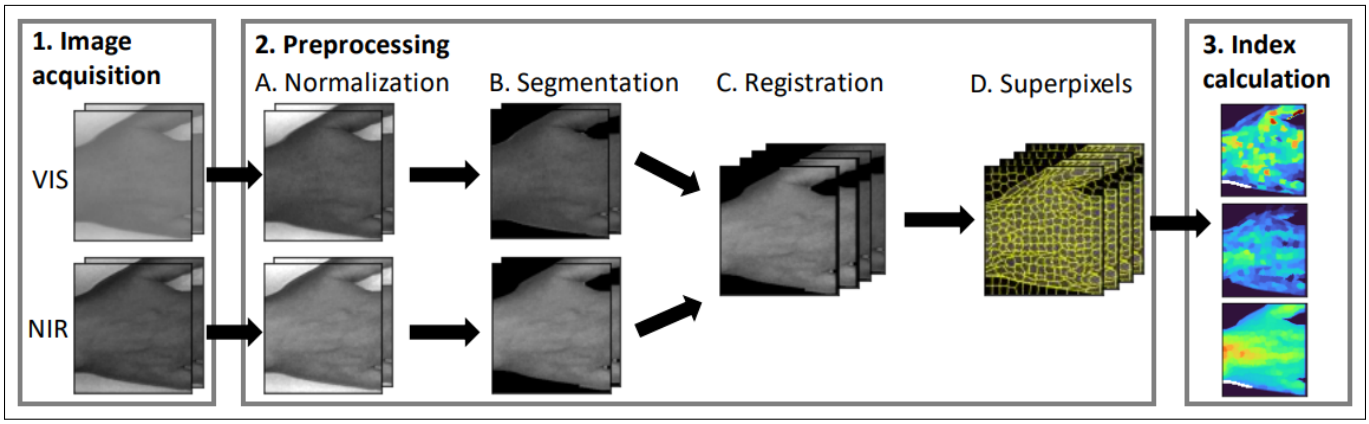

Fig. 1. Illustration of the full pipeline: (1) two hypercubes are captured using a snapshot hyperspectral camera, (2A) the hypercubes are normalized, (2B) the tissue is segmented from the hypercubes, (2C) the VIS and NIR cubes are registered, (2D) the full hypercube is divided into superpixels and finally (3) the various indices are calculated.

D. Ischemia Indices

The computation of the indices was always done per superpixel. This results in a 2D image of superpixels, where each superpixel contains a single value, the index. The images using the desk lamp are used as training and validation, while the LED images are used as a test set. The super pixels of images acquired before and during cuffing are labeled as healthy and ischemic respectively.

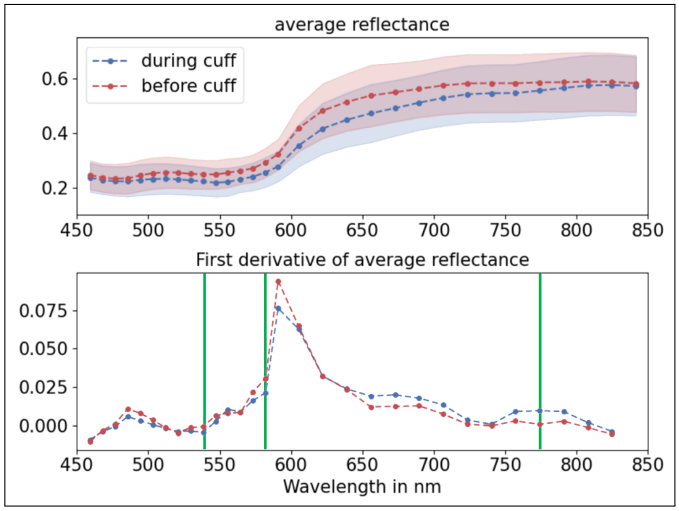

Fig. 2. Absolute reflectance (top) and its first derivative (bottom)

In figure 2, the top graph shows the average reflectance per waveband and its standard deviation for all 12 test subjects of the desk lamp experiment. The bottom graph displays the first derivative of these values. It was decided to work purely with derivative values as these are less dependent on the light source and normalization.

In the following section, R_X, R'_X, A_X and A''_X respectively denote the absolute reflectance, the first derivative of the reflectance, the absolute absorption and the second derivative of the absorption at waveband(s) X.

Using SKLearn's recursive feature selection and a maximum of 4 wavebands, the first derivatives at wavebands 538nm, 582nm and 774nm were found to be able to distinguish best between healthy and ischemic conditions on the train/validation set. Based on this, the following index was designed

$$I_1 = R'_{538} + R'_{582} - 2 \cdot R'_{774}$$

Five indices from other works were compared to the proposed novel index. The wavebands available in this work do not exactly match the ones used in these other works. In these cases, either the nearest wavelength (if the mismatch was smaller than 3 nm) or an interpolation of the two nearest wavelengths available in the hypercube was used (the maximal mismatch was 9 nm). The first of the compared indices is from [11], developed to detect ischemia in pig intestines using hyperspectral images. Their index is calculated as follows:

$$I_2 = C(|\text{sum}(R'_{765:830})| + |\text{sum}(R'_{765:830})|)$$

where C is a constant coefficient to normalize the index. Three other comparable indices originate from [12]. Their goal was to design indices for the non-invasive detection of wound perfusion. Their experiment was performed on hyperspectral images of the palmar side of human hands. The first index was

$$I_3 = \frac{\frac{\min(A''_{570:590})}{r1}}{\frac{\min(A''_{570:590})}{r_1} + \frac{\min(A''_{740:780})}{r_2}}$$

Where r values represent normalization constants. The second index that is tested from [12] is:

$$I_4 = \frac{\text{mean}(A_{530:590}) - r_1}{\text{mean}(A_{785:825}) \cdot (r_1 - r_2)}$$

Their third index, which we define as I_5, was analogous to I_4, but using $A_{825:955}$ and $A_{655:735}$ instead. [13] detected deoxygenation in fingers using hyperspectral images of the dorsal side of the hand. They use the following absorbance ratio:

$$I_6 = \frac{|A_{600}|}{|A_{569}|}$$

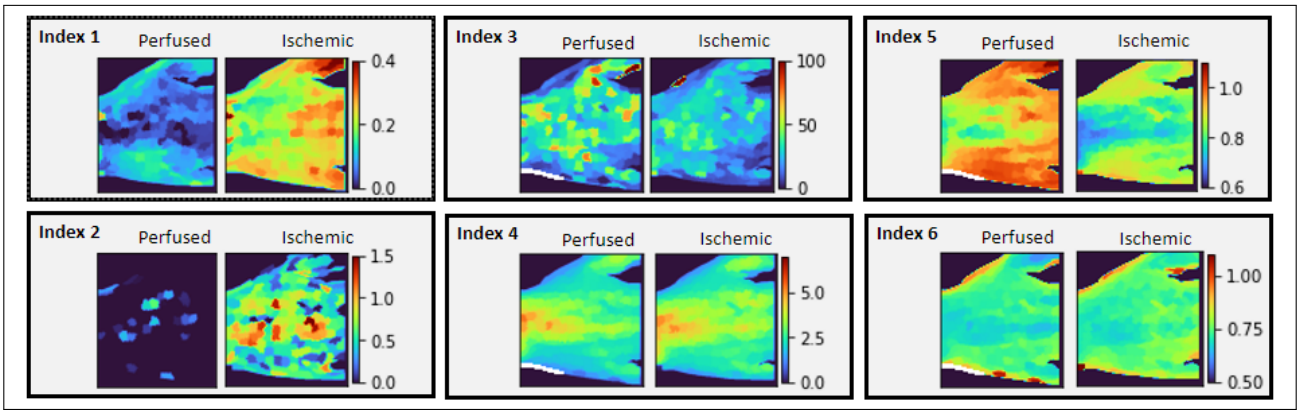

Fig. 3. Perfusion maps of the six different indices. Index 1 represents the novel indices proposed in this work.

III. RESULTS AND DISCUSSION

To test the indices' ability to differentiate between healthy and ischemic tissue, a binary SVM classification was performed on pre- and during-cuffing images, with pre-cuffing labeled as healthy and during-cuffing as ischemic. The various superpixels were used as data samples, i.e. one superpixel corresponds to one input sample containing a single feature, its index value, with their label being either healthy or ischemic. The SVM used had a linear kernel and was not optimized further, as it was essentially used to find an optimal threshold for a single feature. For each index, 12-fold cross validation (alternately using the images of one subject as a validation set) was performed using the desk lamp image data. The 12 SVMs were then each tested using the test set, i.e. the with LED lighting images. As an additional test, for each image, the superpixel index values were averaged out to create a single validation or test sample. The accuracy and standard deviation averaged through all 12 folds are shown in table I.

TABLE I
ACCURACY OF DETECTING HEALTHY VS PERFUSED TISSUE

	Validation Accuracy		Test Accuracy	
Index	Superpixels	Full image	Superpixels	Full image
I_1	$\mathbf{0.87} \pm 0.05$	$\mathbf{1.00} \pm 0.00$	$\mathbf{0.80} \pm 0.03$	$\mathbf{0.96} \pm 0.01$
I_2	0.74 ± 0.09	0.85 ± 0.12	0.50 ± 0.01	0.50 ± 0.00
I_3	0.54 ± 0.06	0.56 ± 0.15	0.52 ± 0.03	0.63 ± 0.16
I_4	0.51 ± 0.06	0.54 ± 0.14	0.49 ± 0.01	0.48 ± 0.07
I_5	0.72 ± 0.08	0.75 ± 0.14	0.62 ± 0.05	0.52 ± 0.07
I_6	0.62 ± 0.07	0.71 ± 0.14	0.53 ± 0.06	0.50 ± 0.00

The results demonstrate that I_1 was the best performing index, with I_1 achieving the highest accuracy in all cases. This index also kept a low standard deviation through all tests, indicating its robustness to different subjects. I_2 and I_5 showed the highest validation accuracy among the five comparable indices. However, the SVM trained on I_5 tended to classify most validation samples of a single participant as part of the same class, while I_2 did not show a clear patient based bias. The classification based on I_3 tended to always predict an ischemic state on the validation full images, resulting in an accuracy of around 50%. Based on superpixels, I_3 showed a patient specific biased, classifying nearly all validation superpixels of a patient as the same class. I_4 was able to classify a few test subjects well but showed severe patient specific bias in some cases. Finally, the SVM trained on I_6 was less dependent on the test subject, but often missclassified healthy tissue as ischemic. As for the test set, the accuracy using proposed index I_1 showed a slight decrease, but still achieved a good performance with 80% on superpixels and 96% on the full images. All other indices, with the exception of I_5 either stayed at or dropped to an accuracy of around 50%. For the test set using the whole hand, only I_3 had an accuracy that wasn't near 50%. In this column, both I_2 and I_6 classified all images as a single class, resulting in a standard deviation of 0.

In figure 3, perfusion index maps of the dorsal side of the hand of a single test subject are shown, with their range set to emphasize differences between healthy and ischemic conditions. It must be emphasized that these images are of a single test subject and thus do not reflect the inter-patient variability. Indices I_1, I_2, and I_5 showed the clearest difference between pre- and during-cuff conditions. However, I_2 had the issue of becoming zero in ischemic cases, which sometimes caused confusion in classification. I_5 values were very dependent on their location, which sometimes caused confusion between healthy and ischemic tissue.

The full pipeline of creating a perfusion map from a HSI hypercube took approximately 1 second on an Intel Core i7 CPU. Furthermore, this time will be shortened further if only the wavebands necessary for the ischemia index are taken into consideration from the start. The use of a GPU would also further enhance the real-time capabilities.

IV. CONCLUSION

In summary, we proposed a new ischemia index for assessing skin tissue perfusion, which was tested on hyperspectral images of the human forearm. The index achieved better classification accuracy compared to five state-of-the-art indices. Furthermore, the proposed index showed to be more robust to changes in lighting. The use of a novel snapshot camera and superpixels enabled real-time imaging and creation of perfusion maps. The development of snapshot HSI cameras that capture only necessary wavebands will further enhance the real-time abilities of ischemia detection with hyperspectral information.

REFERENCES

[1] Hannes Köhler, Boris Jansen-Winkeln, Marianne Maktabi, Manuel Barberio, Jonathan Takoh, Yusef Moulla, Nico Holfert, Michele Diana, Thomas Neumuth, Sebastian Rabe, Claire Chalopin, and Ines Gockel. Evaluation of hyperspectral imaging (hsi) for the measurement of ischemic conditioning effects of the gastric conduit during esophagectomy. *Surgical Endoscopy*, 11 2019.

[2] Gennadi Saiko, Phoebe Lombardi, Yunghan Au, Douglas Queen, David G. Armstrong, and Keith G Harding. Hyperspectral imaging in wound care: A systematic review. *International Wound Journal*, 17:1840 – 1856, 2020.

[3] Jason A. Chin, Edward C. Wang, and Melina R. Kibbe. Evaluation of hyperspectral technology for assessing the presence and severity of peripheral artery disease. *Journal of Vascular Surgery*, 54(6):1679–1688, 2011.

[4] Yun Yu, Yi Lu, Lingzhong Meng, and Ruquan Han. Monitoring cerebral ischemia using cerebral oximetry: Pros and cons. *Journal of biomedical research*, 30, 12 2015.

[5] Jie Hou, Siri Schøne Ness, Jon Tschudi, Marion O'Farrell, Rune Veddegjerde, Ørjan Grøttem Martinsen, Tor Inge Tønnessen, and Runar Strand-Amundsen. Assessment of intestinal ischemia-reperfusion injury using diffuse reflectance vis-nir spectroscopy and histology. *Sensors*, 22(23), 2022.

[6] Leah B Kosyakovsky, Peter C Austin, Heather J Ross, Xuesong Wang, Husam Abdel-Qadir, Shaun G Goodman, Michael E Farkouh, Ruth Croxford, Patrick R Lawler, John A Spertus, and Douglas S Lee. Early invasive coronary angiography and acute ischaemic heart failure outcomes. *European Heart Journal*, 42(36):3756–3766, 07 2021.

[7] Guolan Lu and Baowei Fei. Medical hyperspectral imaging: a review. *Journal of Biomedical Optics*, 19, 2014.

[8] Maria Ewerlöf, Marcus Larsson, and E. Göran Salerud. Spatial and temporal skin blood volume and saturation estimation using a multispectral snapshot imaging camera. In *BiOS*, 2017.

[9] Evgeny Zherebtsov, Viktor Dremin, Alexey Popov, Alexander Doronin, Daria Kurakina, Mikhail Kirillin, Igor Meglinski, and Alexander Bykov. Hyperspectral imaging of human skin aided by artificial neural networks. *Biomed. Opt. Express*, 10(7):3545–3559, Jul 2019.

[10] Radhakrishna Achanta, Appu Shaji, Kevin Smith, Aurelien Lucchi, Pascal Fua, and Sabine Süsstrunk. Slic superpixels compared to state-of-the-art superpixel methods. *IEEE Transactions on Pattern Analysis and Machine Intelligence*, 34(11):2274–2282, 2012.

[11] Hamed Akbari, Yukio Kosugi, Kazuyuki Kojima, and Naofumi Tanaka. Detection and analysis of the intestinal ischemia using visible and invisible hyperspectral imaging. *IEEE Transactions on Biomedical Engineering*, 57:2011–2017, 2010.

[12] Amadeus Holmer, Jörg Marotz, Philip Wahl, Michael Dau, and Peer W. Kämmerer. Hyperspectral imaging in perfusion and wound diagnostics – methods and algorithms for the determination of tissue parameters. *Biomedical Engineering / Biomedizinische Technik*, 63(5):547–556, 2018.

[13] Amadeus Holmer, Florian Tetschke, Jörg Marotz, Hagen Malberg, Wenke Markgraf, Christine Thiele, and Axel Kulcke. Oxygenation and perfusion monitoring with a hyperspectral camera system for chemical based tissue analysis of skin and organs. *Physiological Measurement*, 37(11):2064, oct 2016.